Available online at www.sciencedirect.com
SCIENCE DIRECT
Physica D 219 (2006) 1–12
PHYSICA D
www.elsevier.com/locate/physd

Wave turbulence and vortices in Bose–Einstein condensation

Sergey Nazarenko[a], Miguel Onorato[b,*]

[a] *Mathematics Institute, The University of Warwick, Coventry, CV4 7AL, UK*
[b] *Dipartimento di Fisica Generale, Università di Torino, Via P. Giuria, 1-10125 Torino, Italy*

Received 25 July 2005; received in revised form 6 April 2006; accepted 5 May 2006
Available online 3 July 2006
Communicated by A.C. Newell

Abstract

We report a numerical study of turbulence and Bose–Einstein condensation within the two-dimensional Gross–Pitaevsky model with repulsive interaction. In the presence of weak forcing localized around some wave number in the Fourier space, we observe three qualitatively different evolution stages. At the initial stage a thermodynamic energy equipartition spectrum forms at both smaller and larger scales with respect to the forcing scale. This agrees with predictions of the four-wave kinetic equation of the Wave Turbulence (WT) theory. At the second stage, WT breaks down at large scales and the interactions become strongly nonlinear. Here, we observe formation of a gas of quantum vortices whose number decreases due to an annihilation process helped by the acoustic component. This process leads to formation of a coherent-phase Bose–Einstein condensate. After such a coherent-phase condensate forms, evolution enters a third stage characterised by three-wave interactions of acoustic waves that can be described again using the WT theory.

Keywords: Bose–Einstein condensation; Weak turbulence; Kinetic equation; Bogoliubov dispersion relation

1. Background and motivation

For dilute gases with large energy occupation numbers the Bose–Einstein condensation (BEC) can be described by the Gross–Pitaevsky (GP) equation [1,2]:

$$\mathrm{i}\,\Psi_t + \Delta\,\Psi - |\,\Psi|^2\,\Psi = \gamma, \tag{1}$$

where Ψ is the condensate "wave function" (i.e. the c-number part of the boson annihilation field) and γ is an operator which models possible forcing and dissipation mechanisms which will be discussed later. Renewed interest in the nonlinear dynamics described by the GP equation is related to relatively recent experimental discoveries of BEC [3–5]. The GP equation also describes light behaviour in media with Kerr nonlinearities. In the nonlinear optics context it is usually called the Nonlinear Schrödinger (NLS) equation.

It is presently understood, in both the nonlinear optics and BEC contexts, that the nonlinear dynamics described by the GP equation is typically chaotic and often non-equilibrium [6–9,11]. Thus, it is best characterised as "turbulence" emphasizing its resemblance to the classical Navier–Stokes (NS) turbulence. On the other hand, the GP model has an advantage over NS because it has a weakly nonlinear limit in which the stochastic field evolution can be represented as a large set of weakly interactive dispersive waves. A systematic statistical closure is possible for such systems and the corresponding theory is called Wave Turbulence (WT) [12]. For small perturbations about the zero state in the GP model, WT closure predicts that the main nonlinear process will be four-wave resonant interaction. This closure was used in [6,8,9] to describe the initial stage of BEC. In the present paper we will examine this description numerically. We report that our numerics agree with the predicted by WT spectra at the initial evolution stage.

It was also theoretically predicted that the four-wave WT closure will eventually fail due to the emergence of a coherent condensate state which is uniform in space [9]. Note that strengthening of nonlinearity and corresponding breakdown of the four-wave closure is important for this, because it was shown in [10] that condensation is impossible in the 2D case described by the four-wave kinetic equation. Whereas it is

* Corresponding author. Tel.: +39 0116707454; fax: +39 011658444.
E-mail address: onorato@ph.unito.it (M. Onorato).

0167-2789/$ - see front matter © 2006 Elsevier B.V. All rights reserved.
doi:10.1016/j.physd.2006.05.007

natural to think that without forcing the nonlinearity may remain forever small for sufficiently small initial conditions, in the presence of forcing the nonlinearity will inevitably become strong due to continuous pumping of particles.

At a later stage the condensate is so strong that the nonlinear dynamics can be represented as interactions of small perturbations about the condensate state. Once again, one can use WT to describe such a system, but now the leading process will be a three-wave interaction of acoustic-like waves on the condensate background [9,11]. Coupling of such acoustic turbulence to the condensate was considered in [13] which allowed us to derive the asymptotic law of the condensate growth. However, this picture relies on assumptions that the system will consist of a *uniform* condensate and *small* perturbations. Neither the condensate uniformity nor the smallness of perturbations have ever been validated before. In the present paper we will examine whether it is true that the late stage of GP evolution can be represented as a system of weakly nonlinear acoustic waves about a strong quasi-uniform condensate. By examining the frequency–wave number Fourier transforms, we do observe waves with frequency in agreement with the Bogoliubov dispersion relation. The width of the frequency spectrum is narrow enough for these waves to be called weakly nonlinear.

An unresolved question in the theory of GP turbulence concerns the stage of transition from the four-wave to the three-wave regimes. This stage is strongly nonlinear and, therefore, cannot be described by WT. However, using direct numerical simulations of Eq. (1), we show that the transitional state involves a gas of annihilating vortices. When the number of vortices reduces so that the mean distance between the vortices becomes greater than the vortex core radius (healing length) the dynamics becomes strongly nonlinear. This corresponds to entering the Thomas–Fermi regime when the mean nonlinearity is greater than the dispersive term in the GP equation. The mean inter-vortex distance is a measure of the correlation length of the phase of Ψ and, therefore, the vortex annihilation corresponds to creation of a coherent-phase condensate. At this point, excitations with wavelengths in between of the vortex-core radius and the inter-vortex distance behave as sound. In this paper, we draw attention to the similarity of this transition process to the Kibble–Zurek mechanism of the second-order phase transition which had been introduced originally in cosmology [14,15].

2. WT closure and predictions

The WT closure is based on the assumptions of small nonlinearity and of random phase and amplitude variables. Here we will report the results which will be of help in our discussion (the interested reader should refer to [12] for the standard derivation or to [16] for further developments).

The staring point in the derivation is the GP equation (1) in a periodic box written in Fourier space:

$$\mathrm{i}\partial_t \hat{\Psi}_k - k^2 \hat{\Psi}_k = \sum_{\alpha,\mu,\nu} \bar{\hat{\Psi}}_\alpha \hat{\Psi}_\mu \hat{\Psi}_\nu \delta^{k\alpha}_{\mu\nu} + \hat{\gamma}_k, \tag{2}$$

where $\hat{\Psi}_j = \hat{\Psi}(\mathbf{k}_j)$, an overbar means complex conjugation, wave vectors $\mathbf{k}_j$ $(j = 1, 2, 3)$ are on a 2D grid (due to periodicity) and the term $\delta^{k\alpha}_{\mu\nu} = 1$ for $\mathbf{k} + \mathbf{k}_\alpha = \mathbf{k}_\mu + \mathbf{k}_\nu$ and equal to 0 otherwise.

2.1. Four-wave interaction regime

In order to describe the WT theory for Eq. (2) it is usual to neglect the forcing and dissipation term $\hat{\gamma}_k$ assuming that these are localized at high or low wave numbers and we are mainly interested in an inertial range of $\mathbf{k}$. The goal is to write an evolution equation for the spectrum defined as $\langle \Psi_i \Psi^*_j \rangle = n(\mathbf{k}_i)\delta(\mathbf{k}_i - \mathbf{k}_j)$, where the angle brackets stand for ensemble averages. In order to write such equation it is necessary to exploit small nonlinearity and use a random phase approximation [12] (see also [16] for a generalization of the random phase approximation also to randomness of the amplitudes). The procedure allows us to close equations for the spectrum by using the Wick-type splitting of the higher Fourier moments in terms of the spectrum. In the leading order in nonlinearity one gets the nonlinear frequency correction,

$$\omega_{NL} = 2\int n_k \mathrm{d}\mathbf{k}. \tag{3}$$

The next order gives an evolution equation for the spectrum,

$$\dot{n}_k = 4\pi \int n_k n_u n_\mu n_\nu \times \left(\frac{1}{n_k} + \frac{1}{n_u} - \frac{1}{n_\mu} - \frac{1}{n_\nu}\right) \delta(\omega^{ku}_{\mu\nu}) \delta^{ku}_{\mu\nu}\, \mathrm{d}\mathbf{k}_u \mathrm{d}\mathbf{k}_\mu \mathrm{d}\mathbf{k}_\nu. \tag{4}$$

This is the wave-kinetic equation (WKE) which is the most important object in the wave turbulence theory (for the GE equation, it was first derived in [7]). It contains Delta functions for four wave vectors, $\delta^{ku}_{\mu\nu} = \delta(\mathbf{k} + \mathbf{k}_u - \mathbf{k}_\mu - \mathbf{k}_\nu)$, and for the four corresponding frequencies, $\delta(\omega^{ku}_{\mu\nu}) = \omega_k + \omega_u - \omega_\mu - \omega_\nu$, which means frequencies, $\delta(\omega^{ku}_{\mu\nu})$, which means that the spectrum evolution in this case is driven by a four-wave resonance process. Note that the WT approach is applicable not only to the spectra but also to the higher moments and even the probability density functions [16,17]. However, we are not going to reproduce these results because their study is beyond the aims of the present paper.

As is well known from [12], there are typically four power-law solutions of the four-wave kinetic equation (4) and they are related to the two invariants for such systems, the total energy, $E = \int \omega_k n_k \mathrm{d}\mathbf{k}$, and the total number of particles, $N = \int n_k \mathrm{d}\mathbf{k}$. Two of such power-law solutions correspond to a thermodynamic equipartition of one of these invariants,

$$n_k \sim 1/\omega_k = k^{-2} \quad \text{(energy equipartition)}, \tag{5}$$

$$n_k = \text{const} \quad \text{(particle equipartition)}. \tag{6}$$

These two solutions are limiting cases of the general thermodynamic distribution,

$$n_k = T/(\omega_k + \mu), \tag{7}$$

where constants T and μ have the meanings of temperature and chemical potential respectively. Due to isotropy, it is convenient to deal with an angle-averaged 1D wave action density in

variable $k = |\mathbf{k}|$, the so-called 1D wave action spectrum $N_k = 2\pi k n_k$. In terms of N_k, solutions (5) and (6) have exponents -1 and 1 respectively.

The other two power-law solutions correspond to a Kolmogorov-like constant flux of either energy (down-scale cascade) or the particles (up-scale cascade) [9]. As shown in [9], the formal solution for the inverse cascade has the wrong sign of the particle flux and is, therefore, irrelevant. On the other hand, the power exponent of the direct cascade solution formally coincides with the energy equipartition exponent -2 and, in fact, it is the same solution. Because of such a coincidence, the energy flux value is equal to zero on such a solution and, therefore, it is more appropriate to associate it with thermodynamic equilibrium rather than a cascade.

2.2. Three-wave interaction regime

If the system is forced at large wave numbers and there is no dissipation at low k's then there will be condensation of particles at large scales. The condensate growth will eventually lead to a breakdown of the weak nonlinearity assumption [9,19] and the four-wave WKE (4) will become invalid for describing subsequent evolution. On the other hand, it was argued in [9] that such late evolution one can consider small disturbances of coherent condensate state $\Psi_0 = \text{const}$, so that a WT approach can be used again (but now on a finite-amplitude background),

$$\Psi(\mathbf{x}, t) = \Psi_0 (1 + \phi(\mathbf{x}, t)), \quad \phi \ll \Psi_0. \tag{8}$$

Then, with respect to condensate perturbations ϕ, the linear dynamics has to be diagonalised via the Bogoliubov transformation, which in our case is [9,13,18]

$$\hat{\phi}_k = \frac{1}{2\sqrt{\rho_0}} \left[\left(\frac{k}{\omega_k^{1/2}} + \frac{\omega_k^{1/2}}{k} \right) a_k + \left(\frac{k}{\omega_k^{1/2}} + \frac{\omega_k^{1/2}}{k} \right) \bar{a}_k \right], \tag{9}$$

where a_k are new normal amplitudes (see for example [13]) and $\rho_0 = |\Psi_0|^2$. In the linear approximation, amplitudes a_k oscillate at frequency

$$\omega_k = k\sqrt{k^2 + 2\rho_0} \tag{10}$$

which is called the Bogoliubov dispersion relation. For strong condensate, $\rho_0 \gg k^2$, this dispersion relation corresponds to sound.

Because of the non-zero background, the nonlinearity will be quadratic with respect to the condensate perturbations and, thus, the resulting WT closure now gives rise to a three-wave WKE. This WKE was first obtained in [9] (see also [13]) and here we reproduce it without derivation,

$$\dot{n}_k = \pi \int (R_{k12} - R_{1k2} - R_{2k1})\, \mathrm{d}\mathbf{k}_1 \mathrm{d}\mathbf{k}_2, \tag{11}$$

where

$$R_{k12} = |V_{kk_1k_2}|^2\, \delta(\mathbf{k} - \mathbf{k_1} - \mathbf{k_2})$$
$$\delta(\omega_k - \omega_1 - \omega_2)\, (n_1 n_2 - n_k n_1 - n_k n_2).$$

Here, V_{k,k_1,k_2} is the interaction coefficient which can be found in [9,13].

At late time the condensate becomes strong, $\rho_0 \gg k^2$, and turbulence becomes of acoustic type. The number of particles is not conserved by the turbulence alone (particles can be transferred to the condensate) and there are only two relevant power-law solutions in this case: thermodynamic equipartition of energy and the energy cascade spectrum. Because of isotropy, one often considers 1D (i.e. angle-integrated) energy density,

$$E(k) = 2\pi k \omega_k n_k. \tag{12}$$

In terms of this quantity, the thermodynamic spectrum is

$$E(k) \sim k, \tag{13}$$

and the energy cascade spectrum is

$$E(k) \sim k^{-3/2}. \tag{14}$$

Note that the energy cascade is direct and the corresponding spectrum can be expected in k's higher than the forcing wave number, whereas the thermodynamic spectrum is expected at the low-k range to the left of the forcing [13].

Note that the above described picture of acoustic WT relies on two major assumptions.

1. Condensate is coherent enough so that its spatial variations are slow and it can be treated as uniform when evolution of the perturbations about the condensate is considered. In other words, a scale separation between the condensate and the perturbations occurs.
2. Coherent condensate is much stronger than the chaotic acoustic disturbances. This allows us to treat nonlinearity of the perturbations around the condensate as small.

Both of these assumptions have not been validated before and their numerical check will be one of our goals. Another major goal will be to study the transition stage that lies in between of the four-wave and the three-wave turbulence regimes. This transition is characterised by strong nonlinearity and the role of numerical simulations becomes crucially important in finding its mechanisms.

Once the three-wave acoustic regime has been reached, the condensate continues to grow due to a continuing influx of particles from the acoustic turbulence to the condensate. This evolution, where an unsteady condensate is coupled with acoustic WT, was described in [13] who predicted that asymptotically the condensate grows as $\rho_0 \sim t^2$ if the forcing is of an instability type $\hat{\gamma} = \nu_k n_k$. However, in the present paper we work with a different kind of forcing which is most convenient and widely used in numerical simulations: we keep amplitudes in the forcing range fixed (and we chose their phases randomly). Thus, one should not expect observing the t^2 regime predicted in [13] in our simulations. Note that 2D NLS turbulence was simulated numerically with specific focus on the condensate growth rate in [20]. In our work, we do not aim to study the condensate growth rate because it is strongly dependent on the forcing type which, in our model, is quite different from turbulence sources in laboratory. On the other hand, we believe that the main stages of the

condensation, i.e. transition from a four-wave process, through vortex annihilations, to three-wave acoustic turbulence, are robust under a wide range of forcing types.

3. Setup for numerical experiments

In this paper we consider a setup corresponding to homogeneous turbulence and, therefore, we ignore finite-size effects due to magnetic trapping in BEC or to the finite beam radii in optical experiments. For numerical simulations, we have used a standard pseudo-spectral method [21] for the 2D Eq. (1): the nonlinear term is computed in physical space while the linear part is solved exactly in Fourier space. The integration in time is performed using a second-order Runge–Kutta method. The number of grid points in physical space was set to $N \times N$ with $N = 256$. Resolution in Fourier space was $\Delta k = 2\pi/N$. A sink at high wave numbers was provided by adding to the right hand side of Eq. (1) the hyper-viscosity term $\nu(-\nabla^2)^n \Psi$. Values of ν and n were selected in order to localize as much as possible dissipation to high wave numbers but avoiding at the same time the bottleneck effect. We have found, after a number of trials, that $\nu = 2 \times 10^{-6}$ and $n = 8$ were good choices for our purposes. In some simulations, we have also used a dissipation at low wave numbers of the form of $\nu(-\nabla^2)^{-n} \Psi$ with $\nu = 1 \times 10^{-18}$ and $n = 8$. This was done, e.g., to see what changes if one suppresses the condensate formation. Forcing was localized in Fourier space and was chosen as $f = |f| \exp[-\mathrm{i}\phi(t)]$ with $|f|$ constant in time and $\phi(t)$ randomly selected between 0 and 2π each time step. (i) To study turbulence in the down-scale inertial range we force the system isotropically at wave numbers $4\Delta k \leq |k| \leq 6\Delta k$. To avoid condensation at large scales we introduce a dissipation at low wave numbers, as was previously explained. The forcing was selected as $|f| = 2.1 \times 10^{-3}$. (ii) To study the condensation we chose forcing at wave numbers $60\Delta k \leq |k| \leq 63\Delta k$ and dissipation at all higher wave numbers; in this case $|f| = 1.6 \times 10^{-3}$. A number of numerical simulations were performed both with and without dissipation at the low wave numbers. Time step for integration was $t = 0.1$ and usually 1.1×10^5 time steps have been performed for each simulation. This is usually enough for reaching a steady state when dissipation at both high and low wave numbers was placed. Numerical simulations were performed on a PowerPC G5, 2.7 GHz.

4. Numerical results

4.1. Turbulence with suppressed condensation

We start with a state without condensate for which WT predicts four-wave interactions. WKE has two conserved quantities in this case, the energy and the particles, and the directions of their transfer in the scale space must be opposite to each other. Indeed, let us assume that energy flows up-scale and that it gets dissipated at a scale much greater than the forcing scale. This would imply dissipating the number of particles which is much greater than what was generated at the source (because of the factor k^2 difference between the energy and the particle spectral densities). This is impossible in steady state and, therefore, energy has to be dissipated at smaller (than forcing) scales. On the other hand, the particles have to be transferred to larger scales because dissipating them at very small scales would imply dissipating more energy than produced by forcing. This speculation is standard for the systems with two positive quadratic invariants, e.g. 2D Euler turbulence where one invariant, the energy, flows up-scale and another one, the enstrophy, flows down-scale.

Thus, ideally, one would like to place forcing at an intermediate scale and have two inertial ranges, up-scale and down-scale of the source. However, this setup is unrealistic because the presently available computing power would not allow us to achieve simultaneously two inertial ranges wide enough to study scaling exponents. Therefore, we split this problem in two, with forcing at the left and at the right ends of a single inertial range.

4.1.1. Turbulence down-scale of the forcing

Our first numerical experiment is designed to test the WT predictions about the turbulent state corresponding to the down-scale range with respect to the forcing scale. Thus we chose to force turbulence at large scales and to dissipate it at the small scales as described in the previous section. Our results for the one-dimensional wave action spectrum in statistically stationary condition is shown in Fig. 1. We see a range with slope -1 predicted by both the Kolmogorov–Zakharov (KZ) energy cascade and the thermodynamic energy equipartition solutions of the four-wave WKE. As we mentioned earlier, it would be more appropriate to interpret this spectrum as a quasi-thermodynamic state rather than the KZ cascade because the energy flux expression formally turns into zero at the power spectrum with -1 exponent. We emphasise, however, that the state here is quasi-thermodynamic with a small flux component present on thermal background because of the presence of the source and sink. One could compare this state to a lake with two rivers bringing the water in and out of the lake. In comparison, a pure KZ cascade would be more similar to a waterfall. To check that the waves in our system are indeed weakly nonlinear, we look at the space–time Fourier transform of the wave field. The frequency–wave number plot of this Fourier transform is shown in Fig. 2. We see that this Fourier transform is narrowly concentrated near the linear dispersion curve, which confirms that the wave field is weakly nonlinear. We can also see that the spectrum is slightly shifted upwards by a value which agrees with the nonlinear frequency shift found via substitution of the numerically obtained spectrum into (3).

4.1.2. Up-scale turbulence

In the up-scale range one could expect that, in analogy with the 2D Navier–Stokes turbulence, there would be an inverse cascade of the number of particles and that the corresponding KZ spectrum would be observed. Nevertheless, it was pointed out in [9] that the analytical KZ spectrum has the "wrong" direction of the flux of particles in the 2D GP model and, therefore, cannot form. Our numerics agree with this view. Instead of the KZ, our numerical simulations

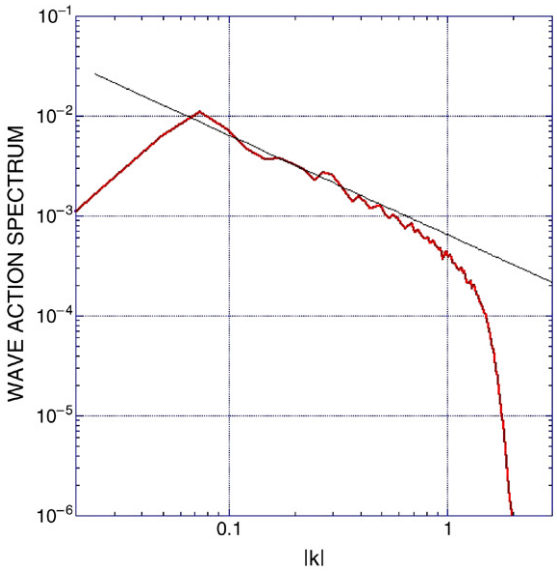

Fig. 1. 1D wave action spectrum N_k for the down-scale inertial range. A line corresponding to k^{-1}, the wave turbulence prediction, is also included.

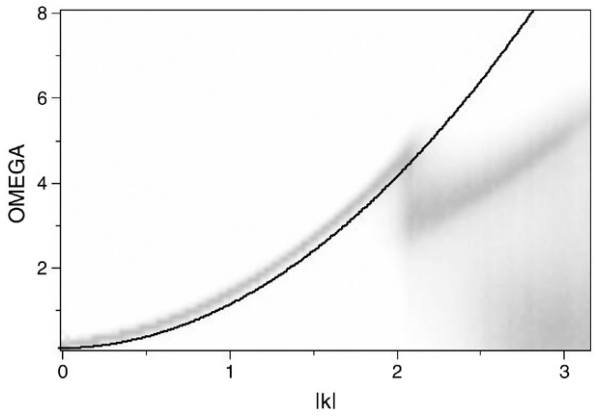

Fig. 2. Wave number–frequency distribution of the space–time Fourier transform of Ψ in the down-scale inertial range. Dispersion relation from linear theory is shown as a black curve.

show that a statistical stationary state with a power law very close to k^{-1} forms, see Fig. 3. This solution corresponds to the thermodynamics solution with energy equipartition in the k-space. Note that both theoretical rejection of the particle-cascade spectrum [9] and our numerical study relate to the 2D model and the situation can change in the 3D case.[1] Namely, it is possible that the up-scale dynamics in 3D will be characterised by the particle-flux KZ solution or a more complicated mixed state which involves both cascade and temperature. On the other hand, formation of a pure thermodynamic state in 2D is quite fortunate for the theoretical description because analogies with the theories of phase transition between different types of thermodynamic equilibria become more meaningful.

[1] Another difference with the 3D case may be that in 3D the condensate can form even at low nonlinearity levels when the four-wave kinetic equation is still valid, whereas this is impossible in 2D [10].

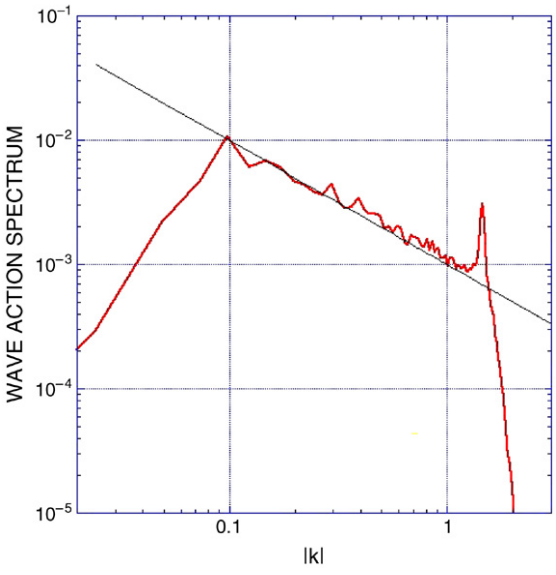

Fig. 3. 1D wave action spectrum N_k in the up-scale range. A power law of the form of k^{-1} is also shown.

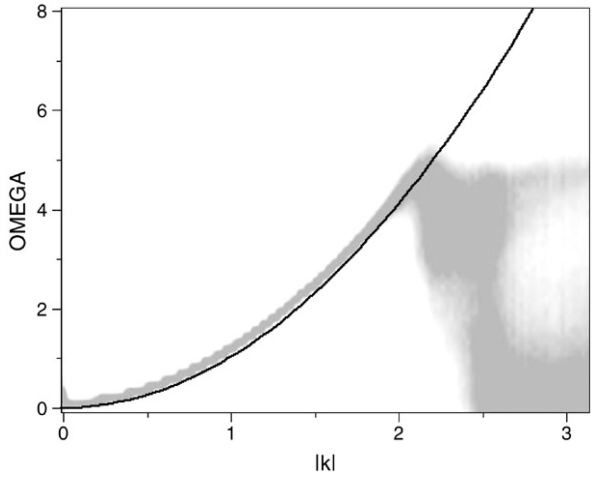

Fig. 4. Wave number–frequency distribution of the space–time Fourier transform of Ψ in the up-scale inertial range. Dispersion relation from linear theory is shown by a black curve.

Here, we also check that the waves in this regime are weakly nonlinear by looking at the space–time Fourier transform. The corresponding frequency–wave number plot is shown in Fig. 4. As in the down-scale inertial range, we see that this Fourier transform is narrowly concentrated near the linear dispersion curve, i.e. the wave field is weakly nonlinear in this state.

4.2. Bose–Einstein condensation

4.2.1. Initial stage: Four-wave process

In order to study the stages of the condensation process, the results presented in the following have been obtained with forcing localized at high wave numbers *without* dissipation at low wave numbers. At the initial stage of the simulation, the nonlinearity remains small compared to the dispersion in the GP equation and the four-wave kinetic equation can be used. In Fig. 5, we show the initial (pre-condensate) stages

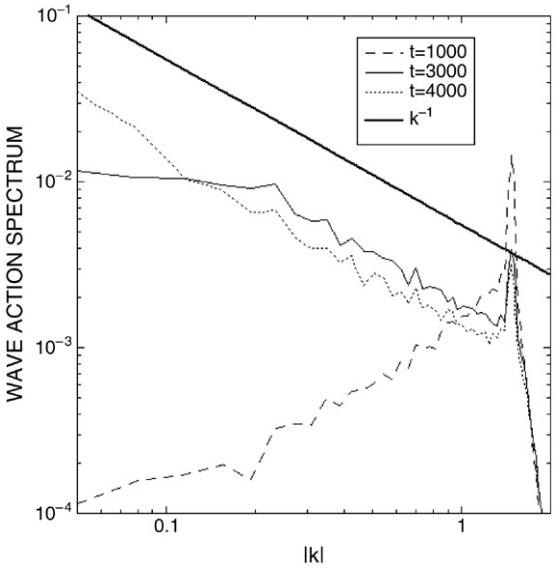

Fig. 5. Initial stages of the evolution of the 1D wave action spectrum N_k. A power law of the form of k^{-1} is also shown.

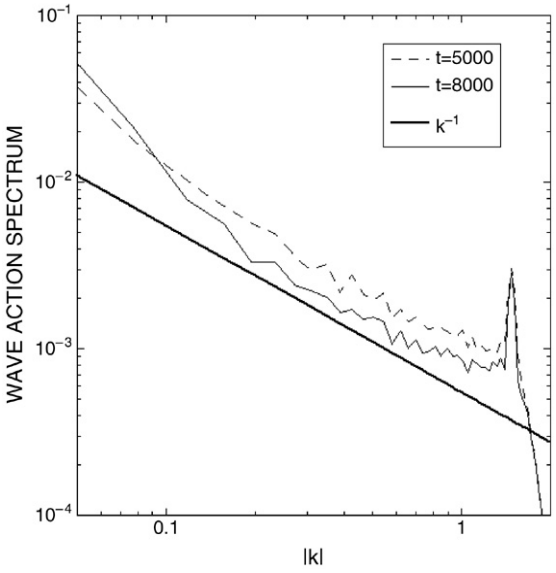

Fig. 6. Later stages of the evolution of the 1D wave action spectrum N_k. A power law of the form of k^{-1} is also shown.

of the spectrum evolution. Similarly to the case where the condensation was suppressed, we observe the formation of a thermodynamic distribution.

4.2.2. Transition

After the stage where the four-wave interaction dynamics holds, the dynamics is characterised by a transitional stage in which the low-k front of the evolving spectrum reaches the largest scale (at about $t = 4000$), see Fig. 6; the spectrum begins to become steeper at low wave numbers and, as expected, the thermodynamics solution does not hold anymore. This behaviour indicates that a change of regime occurs around time $t = 4000$. However, the information contained in the spectrum is insufficient to fully characterize this regime change and this

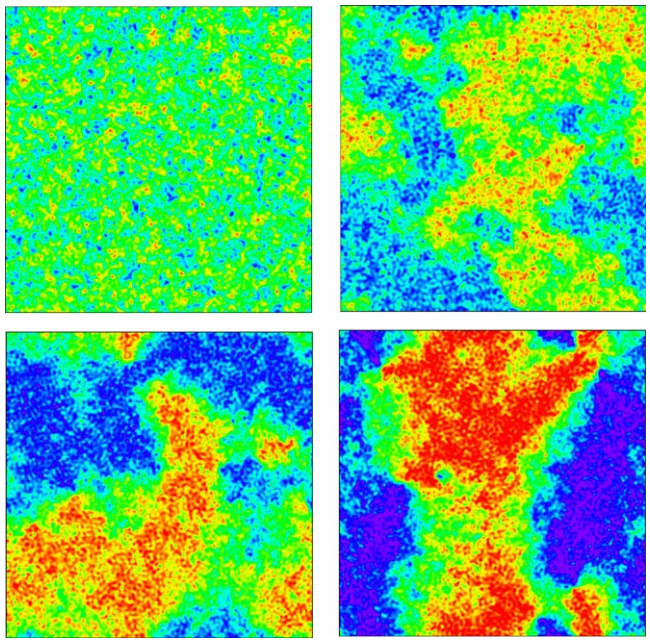

Fig. 7. Re[$\Psi(x, y)$] at different times: $t = 2500$, $t = 5000$, $t = 7500$, $t = 10\,000$.

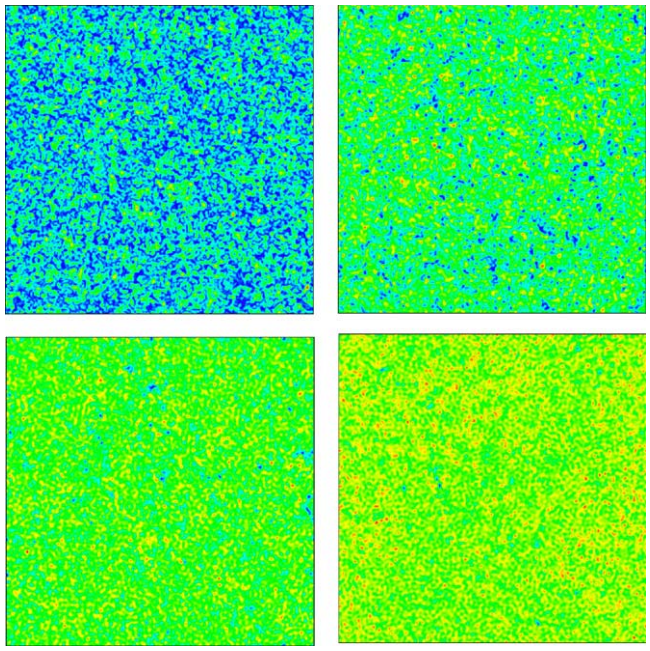

Fig. 8. $|\Psi(x, y)|$ at different times: $t = 2500$, $t = 5000$, $t = 7500$, $t = 10\,000$.

brings us to study this phenomenon by measuring several other important quantities.

To get an initial impression of what is happening during the transition stage it is worth first of all to examine the field distributions in the coordinate space. Fig. 7 shows a series of frames of the real part of Ψ (imaginary part looks similar). One can see that this field exhibits growth of a large-scale structure. On the other hand, a field $|\Psi|$, shown in Fig. 8, still remains dominated by small-scale structure. In contrast with $|\Psi|$, field Ψ contains an additional information — the phase. Thus, separation of the characteristic scales in Figs. 7

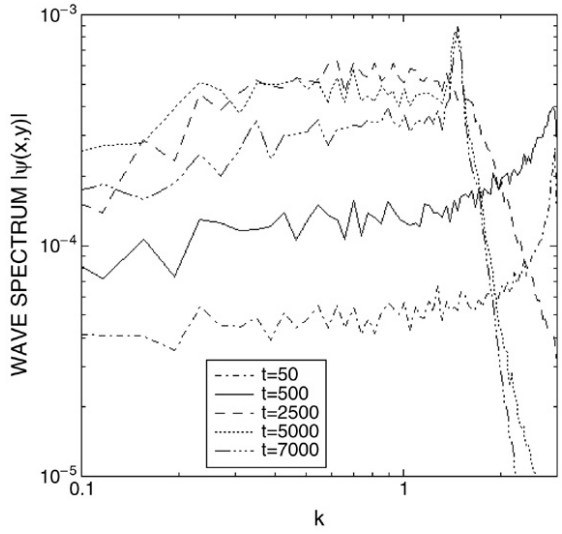

Fig. 9. Spectrum for variable $|\Psi(x, y)|$ at different times.

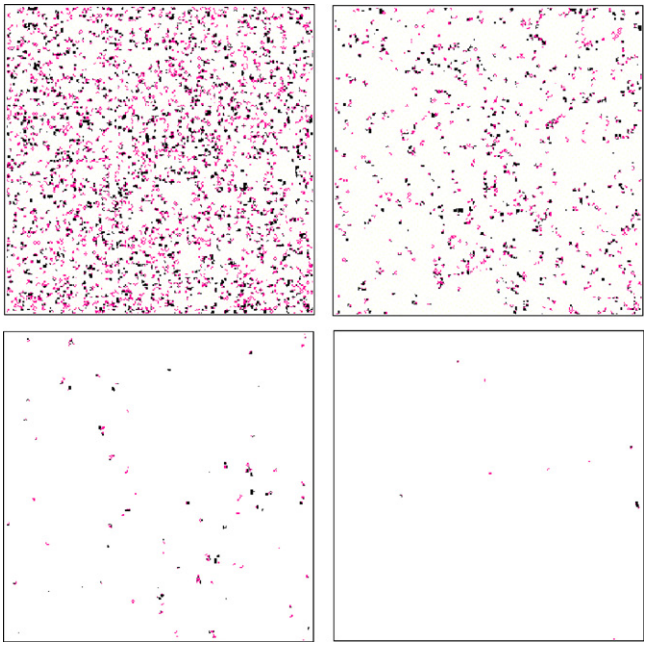

Fig. 10. Vortices in the (x, y) plane at different times: $t = 2500$, $t = 3250$, $t = 5000$, $t = 7500$.

and 8 can be attributed to the fact that the phase correlation length becomes much longer than the typical wavelength of sound (characterised by fluctuations of $|\Psi|$ as explained above in Section 2.2). This scale separation can also be seen by comparing the spectrum of $|\Psi|$, shown in Fig. 9 with the spectrum of Ψ in Figs. 5 and 6: one can see that the former is more flat than the latter. Now that we have established that the phase is an important parameter, we can measure its correlation length as the mean distance between the phase defects — vortices. Vortices in the GP model are points in which $\Psi = 0$. Some of such points correspond to the 2π phase increment when one goes once around them, whereas the other points gain -2π. These vortices can be defined as positive and negative correspondingly. In contrast with the Euler equation of the

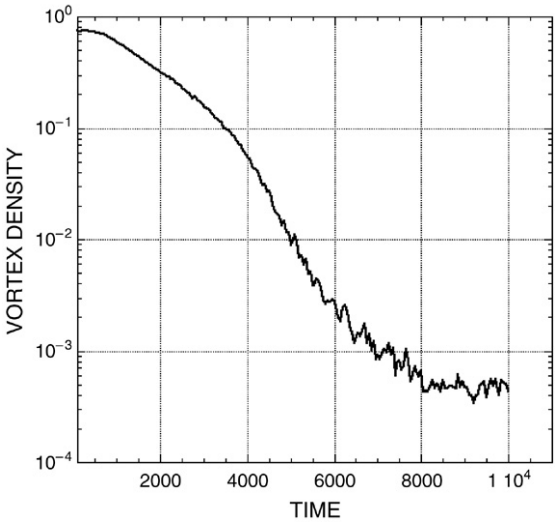

Fig. 11. Evolution in time of the density of vortices in a lin–log plot.

classical fluid, positive and negative vortices can annihilate in the GP model and they can get created "from nothing". Fig. 10 shows a sequence of plates showing the positive and negative vortex positions at several different moments of time. One can see that initially there were a lot of vortices, which is not surprising because the initial field is weak, i.e. close to zero everywhere. However, at later times we see the number of vortices is rapidly dropping, which means that the vortex annihilation process dominates over the vortex-pair creations. The total number of vortices (normalised by N^2) is shown as a function of time in Fig. 11, where one can see a fast decay. The law of decay is best seen on the log–lin plot, see Fig. 12 where one can see a regime

$$N_{\text{vortices}} = A - B \log t \tag{15}$$

with $A = 3.36$ and $B = 0.9223$ which sets in at $t = 800$ to $t = 3500$.[2] Thus, the phase correlation distance, being of the order of the mean distance between the vortices, exhibits a fast growth in time.

A similar picture can be seen if we define the correlation length directly based on the auto-correlation function of field Ψ,

$$C_\Psi(r) = \langle \Psi(\mathbf{x})\, \Psi(\mathbf{x}+\mathbf{r})\rangle / \langle \Psi(\mathbf{x})^2\rangle. \tag{16}$$

Correlation length λ can be defined as

$$\lambda^2 = \int_0^{r_0} C_\Psi(r)\, \mathrm{d}\mathbf{r}, \tag{17}$$

where r_0 is the first zero of $C_\Psi(r)$.[3] Fig. 13 shows evolution of $1/\lambda^2$ which, as we see, has a similar trend as the one in Fig. 12 (showing the same quantity based on the inter-vortex spacing

[2] At present, we do not have a theoretical explanation of this law of decay.

[3] Strictly speaking, $C_\Psi(r)$ can strongly oscillate, particularly at the initial stages characterised by weakly nonlinear waves, i.e. the correlation length is longer than the one defined based on the first zero. However, only *positive* correlation is relevant to the condensate, which explains our definition of λ.

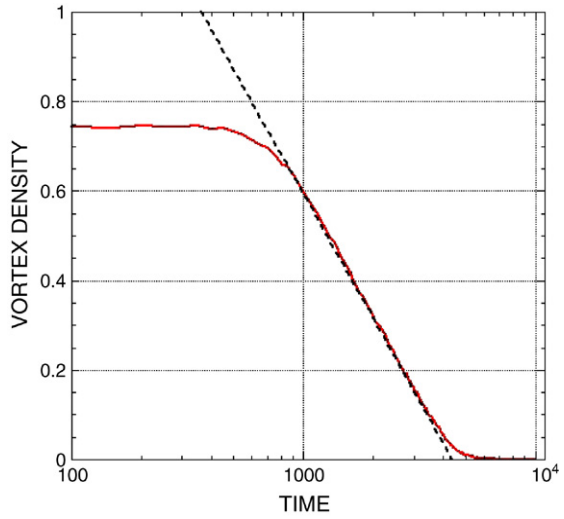

Fig. 12. Evolution in time of the density of vortices in a log–lin plot. The dashed line corresponds to the fit $N_{\text{vortices}} = 3.36–9.223\text{Log}(t)$.

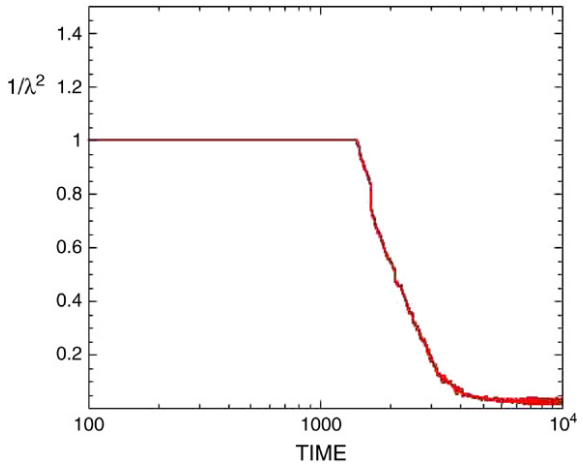

Fig. 13. Evolution in time of the correlation length.

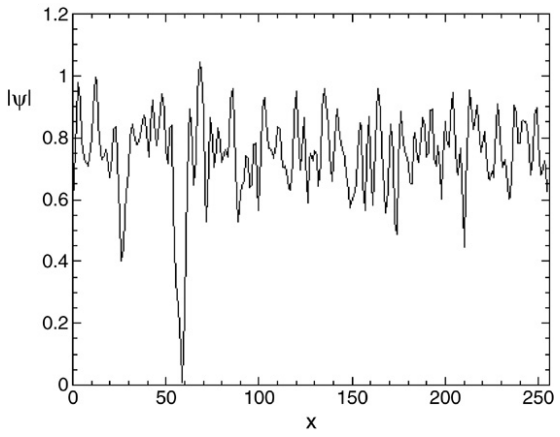

Fig. 14. Slice of the field $|\Psi|$ for constant y: a single vortex is visible in the plot.

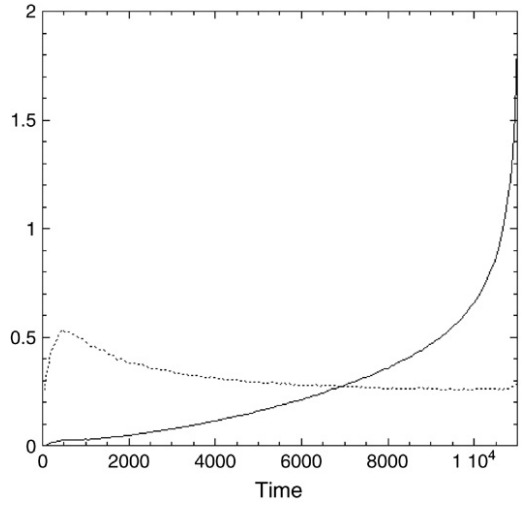

Fig. 15. The solid line represents the space-averaged $|\nabla^2 \Psi(x, y)|$; the dotted line is the space-averaged $|\Psi(x, y)|^3$. See text for comments.

definition of the correlation length). Let us have a look at a slice of the field $|\Psi|$ through typical vortices at a late time when most of them have annihilated, see Fig. 14. One can see that $|\Psi|$ is close to zero (i.e. both Re$[\Psi]$ and Im$[\Psi]$ cross zero) at the vortex centres and that it sharply grows to order-one values ("heals") at small distances from the vortex centres which are much less than the distance between the vortices. This means that these vortices represent fully nonlinear coherent structures, each of which can be approximately seen as an isolated Pitaevsky vortex solution [2]. In contrast, the initial vortices are too close to each other to be coherent and they correspond to a nearly linear field.[4] The moment when the mean inter-vortex separation becomes comparable to the healing length can be captured by the intersection point of the graphs for the mean (space averaged) nonlinear and the mean (space averaged) Laplacian terms in the GP equation, see Fig. 15. This intersection (at $t = 6950$) marks the moment when mean nonlinearity becomes greater than the mean linear dispersion, i.e. the Thomas–Fermi regime sets in. This regime could be thought of as the one of a fully developed condensate when the nonlinearity, when measured with respect to the zero level, is strong and therefore the four-wave WT description breaks down. However, as we will see in the next section, we now have weakly nonlinear perturbations if they are measured with respect to a non-zero condensate state. Evolution of such perturbations takes the form of three-wave acoustic turbulence.

What makes vortices annihilate? A positive–negative vortex pair, when taken in isolation, would propagate with constant speed without changing the distance between the vortices [25]. Thus, there should be an additional entity which could exchange energy and momentum with the vortex pair and to allow them to annihilate. We note that the field $|\Psi|$ is very "choppy" in the region between the vortices, see (Fig. 14), and, therefore, it is natural to conjecture that the missing entity is sound. To check this conjecture, we perform the following numerical experiment. At a desired time we filter the field and let it evolve further without sound. The filtering is performed numerically in the following way: we have used a Gaussian filter in physical space and have smoothed the field around

[4] For this reason such vortices are sometimes called "ghost vortices" [22].

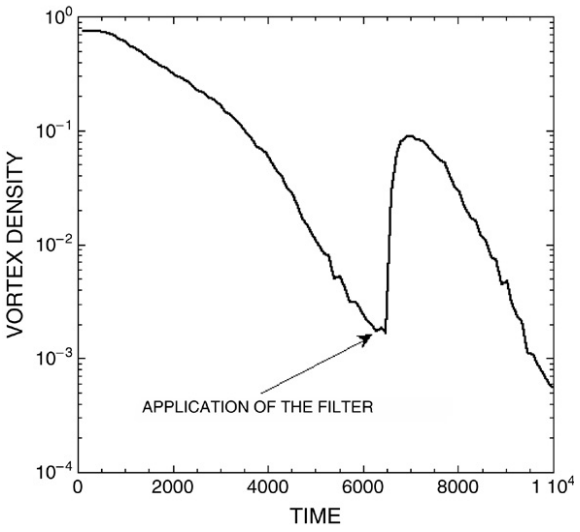

Fig. 16. Evolution of the vortex density in time. At time $t = 6500$, sound has been filtered according to the methodology described in the text.

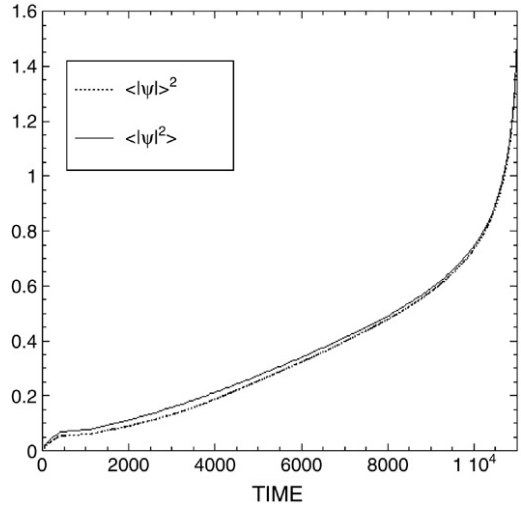

Fig. 17. Evolution in time of $\langle|\Psi|^2\rangle$ and $\langle|\Psi|\rangle^2$.

vortices. The complex field Ψ is therefore convoluted with a normalised Gaussian function with standard deviation much smaller with respect to the mean distance between vortices. The filter is applied only in the region where no vortices are located. The result of the filtering procedure on the evolution of the number of vortices is shown in Fig. 16. We see that removing the sound component does indeed reverse the vortex annihilation process and for some time (until new sound gets generated from forcing) we observe that the vortex creation process dominates. We point out that the described above regime change, accompanied by vortex annihilations, is very similar to the Kibble–Zurek mechanism of the second-order phase transition [14,15]. This mechanism, originally developed in cosmology, suggest that at an early inflation stage, Higgs fields experience a symmetry breaking transition from "false" to "true" vacuum, and this transition is accompanied by a reconnection–annihilation of "cosmic strings" which are 3D analogs of the 2D point vortices considered in this paper. To describe these fields, one normally uses nonlinear equations of the so-called Abelian model [23], but the non-linear Klein-Gordon or even the GP equation are sometimes used as simple models in cosmology which retain similar physics [23,24].

4.2.3. Late condensation stage: Acoustic turbulence

It was predicted in [9] that the turbulent condensation in the GP model will lead to creation of a strong coherent mode with $k = 0$ such that the excitations at higher wave numbers would be weak compared to this mode. If this is the case, one can expand the GP equation about the new equilibrium state, uniform condensate, use the Bogoliubov transform to find new normal modes and a dispersion relation for them, Eq. (9), and to obtain a new WKE for this system that would be characterised by three-wave interactions, (11). However, as we saw in Fig. 6 the peak at small k remains quite broad, that is the coherent condensate, if present, remains somewhat non-uniform. Despite this non-uniformity, one can still use the approach of [9] if there is a scale separation between the condensate coherence length (intervortex distance) and the sound wavelength and if the sound amplitude is much smaller than the one of the condensate.

We have already seen a tendency to the scale separation in Figs. 6–9. On the other hand, smallness of the sound intensity can be seen in Fig. 17 which compares (space-averaged) $\langle|\Psi|^2\rangle$ and $\langle|\Psi|\rangle^2$. We see that at the late stages these quantities have very close values which means that the deviations of $|\Psi|$ from its mean value (condensate) are weak. Thus, both conditions for the weak acoustic turbulence to exist are satisfied at the late stages. However, the best way to check if the condensate perturbations do behave like weakly nonlinear sound waves obeying the Bogoliubov dispersion relation consists in plotting the square of the absolute value of the space–time Fourier transform of Ψ. This result is given in Fig. 18 for the latest stage of the simulation (from time $t = 10\,488$ to $t = 11\,000$). Note that for each k the spectrum has been divided by its maximum in order to be able to follow the dispersion relation up to high wave numbers.

The normal variable for the Bogoliubov sound is given in terms of Ψ by expressions (8) and (9), and, therefore, when plotting the Bogoliubov dispersion (10), we should add a constant frequency of the condensate oscillations, $\omega_0 = \langle|\Psi|^2\rangle$. One can see that the main branch of the spectrum does follow the Bogoliubov law up to the wave numbers which correspond to the dissipation range.[5] Further, the wave distribution is quite narrowly concentrated around the Bogoliubov curve which indicates that these waves are weakly nonlinear. However, one should realise that for formal applicability of the three-wave kinetic equation the nonlinear frequency broadening should be less than the dispersion which is strictly speaking not satisfied in Fig. 18 in small k. Thus, it is possible that weak shocks are also present. Note that the lower branch in Fig. 18 is related to the $\bar{a}_k$ contribution to expression (9) which vanishes

[5] At the same time, these wave numbers are of the order of the inverse healing length, and it is unclear whether the Bogoliubov mode is not seen there due to wave dissipation or due to contamination of this range by the broadband (in frequency) vortex motions.

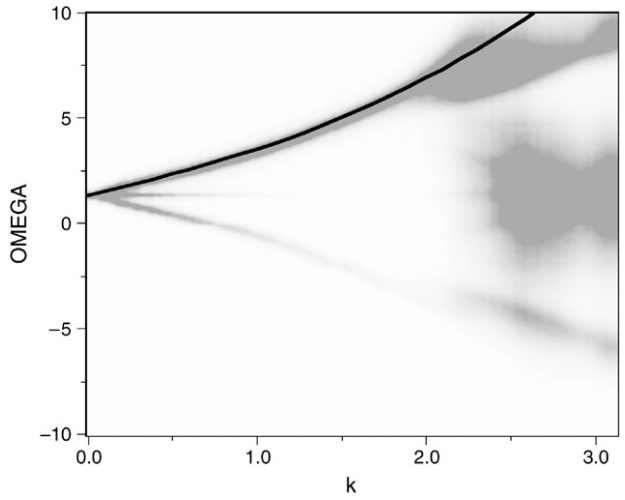

Fig. 18. Dispersion relation calculated from numerical simulation compared with the upper branch of the Bogoliubov dispersion relation (solid line).

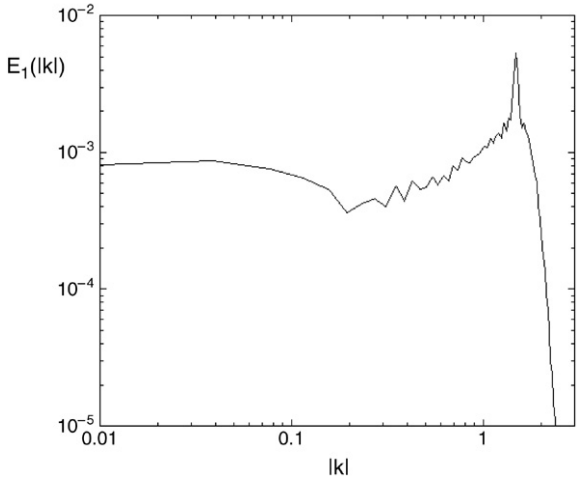

Fig. 19. $E_1(k)$ at the latest stage of the simulation (see Eq. (18)).

at larger k. Importantly, we can also see the middle (horizontal) branch with frequency ω_0 which quickly fades away at finite k's and which corresponds to the coherent large-scale condensate component.

Now let us consider the energy spectrum. The GP Hamiltonian can be written in terms of both real and Fourier quantities,

$$H = \int \left(|\nabla \Psi|^2 + \frac{1}{2} |\Psi|^4 \right) \mathrm{d}\mathbf{x} = \int \left(k^2 |\hat{\Psi}|^2 + \frac{1}{2} |\hat{\rho}|^2 \right) \mathrm{d}\mathbf{k}, \tag{18}$$

where $\rho = |\Psi|^2$. Thus, we measure the 1D energy spectrum in this case as $E(k) = E_1(k) + E_2(k)$ with $E_1(k) = k^3 |\hat{\Psi}|^2$ and $E_2(k) = \frac{k}{2} |\hat{\rho}|^2$ The contributions to the energy spectrum E_1 and E_2 as well as the total spectrum $E(k)$ at a time corresponding to the acoustic regime are shown in Figs. 19–21 respectively.

We see that at small scales the total energy spectrum $E(k)$ scales as $1/k$ which is a thermodynamic energy equipartition solution in this case.

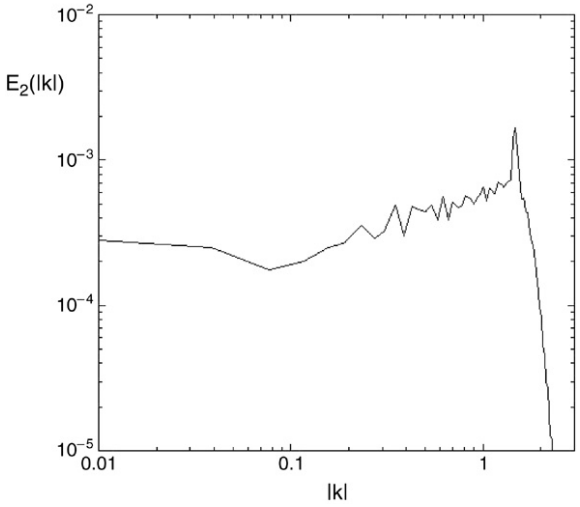

Fig. 20. $E_2(k)$ at the latest stage of the simulation (see Eq. (18)).

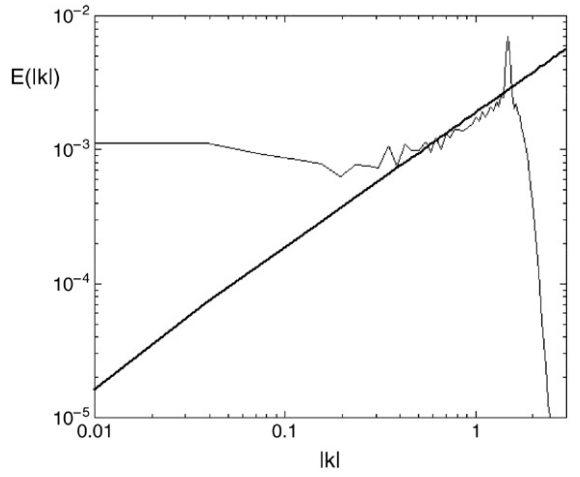

Fig. 21. $E(k) = E(k_1) + E(k_2)$ at the latest stage of the simulation (see Eq. (18)).

4.2.4. *Frustration of condensation by sound absorption*

We showed above that sound is important for the vortex annihilation and, therefore, for the condensation process. Does it mean that in systems where sound absorption is present one can expect frustration of the condensation process? To answer this question we performed numerical experiments with partial sound filtering applied every 100 time steps; namely, each 100 time steps, we have replaced Ψ in the following way:

$$\Psi \to (1 + C)\, \Psi + C\, \tilde{\Psi}, \tag{19}$$

where $\tilde{\Psi}$ is the field obtained from the application of the Gaussian filter described above to the field Ψ. Constant $C \ll 1$ corresponds to the fraction of the sound component which is filtered out each 100 time steps. Such a partial filter could be seen as a simple model for systems which can gradually lose sound via radiation or absorption at the boundaries.

The numerical results for the evolution of the vortex density in time (for different sound absorption coefficients C) are shown in Fig. 22. We see that the sound absorption indeed slows the condensation down and, for sufficiently high absorption,

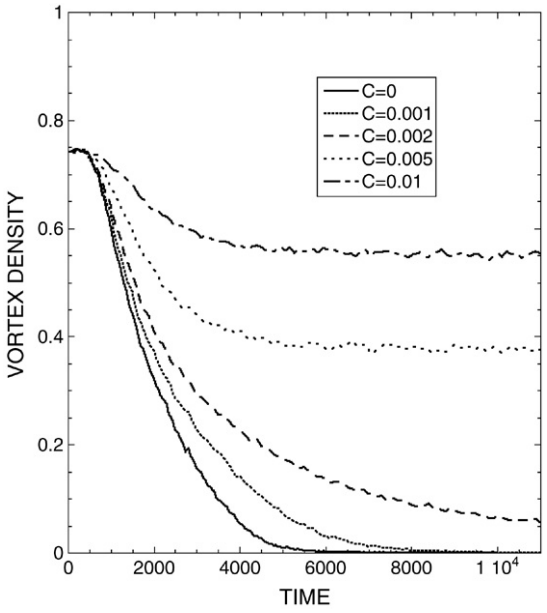

Fig. 22. Evolution in time of the density of vortices for different values of C (see text for details).

it can completely halt the condensation process. Namely, for large C's we see that the vortex density asymptotes to a constant level, which means that the phase coherence length stops growing at a certain finite value.

5. Conclusions

Firstly, we confirmed WT predictions of the energy spectra in the down-scale and up-scale inertial intervals in the cases when the fluxes are absorbed by dissipation at the end of the inertial interval (so that no condensation or build-up is happening). In both of these cases we observed spectra with an exponent corresponding to the energy equipartition thermodynamic solution $N_k \sim 1/k$ (which formally coincides with the exponent for the energy cascade solution). By looking at the shape of the frequency–wave number mode distributions, we verified that the turbulence is weak.

Secondly, we studied a system without dissipation at large scales. We observed a process of Bose–Einstein condensation and formation of a coherent large-scale mode which happens via annihilating vortices. The condensate correlation length, which in our case is of the order of the mean inter-vortex distance, turns into infinity in a finite time as $\lambda \sim 1/(\log t^* - \log t)^{1/2}$, see Eq. (15).

We established that the process of the vortex annihilation is due to the presence of sound. The presence of sound is crucial for creation and maintaining the coherent phase and sound absorption leads to frustration of the perfect condensation. This conclusion may seem counter-intuitive because it implies that perfectly constant coherent condensate (without sound) could not be stable.

We confirmed numerically that in late condensation stages the system can be described as a weakly nonlinear acoustic turbulence on the background of a quasi-uniform coherent condensate. Namely, we confirmed that the wave excitations are narrowly distributed around the Bogoliubov dispersion law, i.e. that the turbulence is (i) acoustic and (ii) weak. We observed a spectrum that corresponds to the energy equipartition solution of the three-wave kinetic equation for such acoustic turbulence.

We would like to stress that the presence of forcing is important for the observed condensation effect, particularly for the presence of the strongly nonlinear stage characterised by annihilating vortices. In the case of decaying turbulence, it is possible that under certain conditions the nonlinearity will never become large and the four-wave WKE will remain valid. In this case, Bose condensation is impossible in 2D, as was shown in [10]. Decaying turbulence, particularly conditions of validity of the four-wave WKE, should be studied separately.

An interesting question to be addressed in the future is to what extent the findings of this work are relevant to the 3D GP model. We can speculate that the energy spectra may have a different nature in 3D and, in particular, may expect formation of the Kolmogorov-like spectra corresponding to the energy and the particle cascades. On the other hand, it is reasonable to expect that the Kibble–Zurek scenario of condensation will persist in the 3D case, i.e. the correlation length will grow because of the reconnecting and shrinking vortex loops. It is also likely that such vortex loop shrinking will be facilitated by the sound component. Computations of 3D GP equation in a non-turbulent setting were done in [26] where such processes such as vortex reconnection and the role of the acoustic component were considered. Turbulent setting will be more taxing on the computing resources due to the great variety of scales involved and, therefore, necessity of high resolution and long computation times.

Acknowledgment

We thank Al Osborne for discussions in the early stages of the work.

References

[1] E.P. Gross, Structure of a quantized vortex in boson systems, Nuovo Cimento 20 (1961) 454.
[2] L.P. Pitaevsky, Vortex lines in an imperfect Bose gas, Sov. Phys. JETP 13 (1961) 451.
[3] M.H. Anderson, J.R. Ensher, M.R. Matthews, C.E. Wieman, E.A. Cornell, Observation of Bose–Einstein condensation in a dilute atomic vapor, Science 269 (1995) 198.
[4] C.C. Bradley, C.A. Sackett, J.J. Tollett, R.G. Hulet, Evidence of Bose–Einstein condensation in an atomic gas with attractive interactions, Phys. Rev. Lett. 75 (1995) 1687–1690.
[5] K.B. Davis, M.-O. Mewes, M.R. Andrews, N.J. van Druten, D.S. Durfee, D.M. Kurn, W. Ketterle, Bose–Einstein Condensation in a gas of sodium atoms, Phys. Rev. Lett. 75 (1995) 3969.
[6] Yu.M. Kagan, B.V. Svistunov, G.P. Shlyapnikov, Kinetics of Bose condensation in an interacting Bose gas, Sov. Phys. JETP 75 (1992) 387.
[7] V.E. Zakharov, S.L. Musher, A.M. Rubenchik, Hamiltonian approach to the description of nonlinear plasma phenomena, Phys. Rep. 129 (1985) 285.
[8] D.V. Semikoz, I.I. Tkachev, Kinetics of Bose Condensation, Phys. Rev. Lett. 74 (1995) 3093–3097.
[9] A. Dyachenko, A.C. Newell, A. Pushkarev, V.E. Zakharov, Optical turbulence: Weak turbulence, condensates and collapsing filaments in the nonlinear Schrödinger equation, Physica D 57 (1992) 96.

[10] C. Connaughton, C. Josserand, A. Picozzi, Y. Pomeau, S. Rica, Condensation of classical nonlinear waves, Phys. Rev. Lett. 95 (2005) 263901. Also http://arXiv.org:cond-mat/0502499, 2005.
[11] Y. Pomeau, Asymptotic time behaviour of nonlinear classical field equations, Nonlinearity 5 (1992) 707–720.
[12] V.E. Zakharov, V.S. L'vov, G. Falkovich, Kolmogorov Spectra of Turbulence, Springer-Verlag, 1992.
[13] V.E. Zakharov, S.V. Nazarenko, Dynamics of the Bose–Einstein condensation, Physica D 201 (2005) 203–211.
[14] T.W.B. Kibble, Topology of cosmic domains and strings, J. Phys. A: Math. Gen. 9 (1976) 1387.
[15] W.H. Zurek, Cosmological experiments in superfluid helium? Nature 317 (1985) 505; Acta Phys. Pol. B24 (1993) 1301.
[16] Y. Choi, Yu. Lvov, S.V. Nazarenko, B. Pokorni, Anomalous probability of large amplitudes in wave turbulence, Phys. Lett. A 339 (3–5) (2004) 361–369. arXiv:math-ph/0404022.
Y. Choi, Yu. Lvov, S.V. Nazarenko, Joint statistics of amplitudes and phases in wave turbulence, Physica D 201 (2005) 121–149.
[17] Yu. Lvov, S. Nazarenko, Noisy spectra, long correlations and intermittency in wave turbulence, Phys. Rev. E 69 (2004) 066608. Also http://arxiv.org/abs/math-ph/0305028, 2004.
[18] Yu.V. Lvov, S. Nazarenko, R. West, Wave turbulence in Bose–Einstein condensates, Physica D 184 (2003) 333–351.
[19] L. Biven, S.V. Nazarenko, A.C. Newell, Breakdown of wave turbulence and the onset of intermittency, Phys. Lett. A 280 (2001) 28–32;
A.C. Newell, S.V. Nazarenko, L. Biven, Physica D 152–153 (2001) 520–550.
[20] A. Dyachenko, G. Falkovich, Condensate turbulence in two dimensions, Phys. Rev. E 54 (1996) 5095.
[21] B. Fornberg, A practical guide to pseudospectral methods Cambridge Monographs on Applied and Computational Mathematics (No. 1), February 1999.
[22] M. Tsubota, K. Kasamatsu, M. Ueda, Vortex lattice formation in a rotating Bose–Einstein condensate, Phys. Rev. A 65 (2002) 023603.
[23] J.A. Peacock, Cosmological Physics, Cambridge University Press, 1999.
[24] W.H. Zurek, Cosmological experiments in condensed matter systems, Phys. Rep. 276 (1996) 177–221.
[25] C.A. Jones, P.H. Roberts, Motions in a Bose condensate. IV. Axisymmetric solitary waves, J. Phys. A: Math. Gen. 15 (1982) 2599.
[26] N.G. Berloff, Interactions of vortices with rarefaction solitary waves in a condensate and their role in the decay of superfluid turbulence, Phys. Rev. A 69 (2004) 053601.